Physical Properties of a New Fractal Model of Percolation Clusters

Benoit B. Mandelbrot and James A. Given
IBM Thomas J. Watson Research Center, Yorktown Heights, New York 10598
(Received 29 December 1983)

We investigate nonrandom, half-random, and random variants of clusters generated by the "squig" process, using renormalization or Monte Carlo methods. Each variant is compared to two-dimensional percolation clusters at criticality from the viewpoints of the fractal dimensionalities of the whole, the backbone, the multiconnected parts, the ring hulls, the backbone links, the shortest paths, and the recurrences of diffusion, hence the fracton dimensionality. The random variant fits very well when its only parameter s is a bit above 0.4.

PACS numbers: 05.40.+j

While our understanding of the physics and geometry of percolation clusters and backbones at criticality has greatly improved, a realistic but manageable recursive model had been lacking. This paper describes the geometrical and physical properties of the fractal "squig clusters" (Ref. 1, Sec. 1.1.1). The squig process (Ref. 2, Chap. 24) is a versatile new method of constructing fractals by recursive interpolation or extrapolation. The word "squig" refers to the "squiggly" appearance of these fractals. The main finding is that the random squig clusters fit very well. Reference 1, Sec. 1.1.8, describes noncritical clusters, but our concern here is solely with critical clusters, which are of interest in themselves and resemble fractal aggregates and other lattice random fractals in physics.

We begin with the nonrandom Koch curve drawn with the generator in Fig. 1(a). Its fractal dimensionality is $\log_3 8 \sim 1.8928$, very close to the known[2,3] percolation value of $2-\beta/\nu$ in two dimensions. Asymptotically, the cluster fills a Sierpinski carpet of base $b=3$. The carpet's midsquare contains another cluster, etc. The backbone between A and B (see Fig. 2) is a Koch curve in this case; its generator, Fig. 1(b), is the backbone of the overall generator; the dimensionality is $\log_3 6$. In the backbone, multiply connected portions, that Ref. 1 calls "rings," alternate with "backbone links" important[4] to the Ising model at low T. Each ring's dimensionality is $\log_3 6$. The backbone links approximate the triadic Cantor set [generator in Fig. 1(c)], of dimensionality $\log_3 2$. For each ring, the hull boundary[1,2] is made of the bonds accessible to paths from the outside. Its generator is either Fig. 1(d) or Fig. 1(e), of dimensionality $\log_3 5$. Now consider a random ant on our cluster, as an example of "ant in a fractal labyrinth."[5-9] By the renormalization technique in Ref. 6, the mean square displacement after n steps is n^{2H}, with $2H=\log 9/\log 22$. Thus, the dimensionality of the walk's trail is $d_w=1/H=\log_3 22$. Because $d_w > \log_3 8$, our random walk self-overlaps repeatedly. Thus, d_w is a "latent" dimensionality in the sense of Ref. 1 (Sec. 2.1), while the actual fractal dimensionality is $\log_3 8$. By Refs. 7 and 8 or the rules in Ref. 1 (Table I), the fractal dimensionality of this walk's recurrences to the origin is $1-H\log_3 8 = 1-\log_{22} 8$, and the (spectral) fracton dimensionality (twice the codimensionality of recurrence) is $\log_{22} 64$. Shortest paths are of dimensionality $\log_3 3$.

In Table I, column 2 shows estimated dimensionalities for the two-dimensional percolation cluster at criticality. Column 3 reports on the new nonrandom model. The fit is rough, but not unreason-

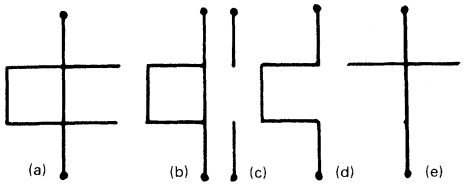

FIG. 1. Generators of several Koch curves: (a) our nonrandom cluster; (b) its backbone; (c) its backbone links; (d),(e) its rings' hull boundary.

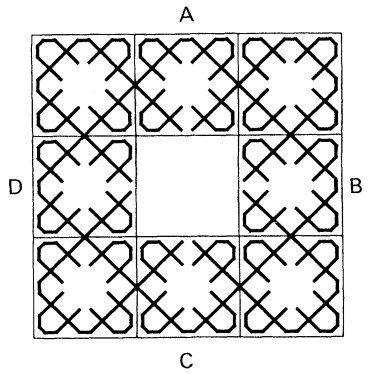

FIG. 2. Second stage of construction of a Koch curve drawn with use of a square initiator $ABCD$ and the generator in Fig. 1(a). The allowed crossings of sites are marked.

TABLE I. Comparison of fractal dimensionalities of different portions of two-dimensional percolation clusters at criticality and of Ref. 1 clusters.

	Percolation in the plane at criticality	Ref. 1 clusters		
		Nonrandom	Half-random $s=0.4$	Random $s=0.4$
(1) Whole cluster	$2-\beta/\nu \sim 1.89$[a]	$\log_3 8 \sim 1.8928$	$\log_3 8 \sim 1.8928$	$\log_3 8 \sim 1.8928$
(2) Ring or backbone	1.6–1.71[b]	$\log_3 6 \sim 1.6309$[c]	1.724[c]	1.716[c]
(3) Ring's hull boundary	1.38[d]	$\log_3 5 \sim 1.4650$[c]	1.403[c]	$1.36 << 1.40$[e]
(4) Backbone links	$1/\nu \sim 75$[f]	$\log_3 2 \sim 0.6309$[c]	0.682[c]	0.739[c]
(5) Random walk's trail	2.835[g]	$\log_3 22 \sim 2.815$[c]	2.789[h]	2.829[h]
(6) Recurrences to origin	1/3[i]	$1-\log_{22} 8 \sim 0.3272$[j]	0.320[j]	0.331[j]
(7) D_{fracton}	$\sim 4/3$[k]	$\log_{22} 64 \sim 1.3454$[j]	1.360[j]	1.338[j]
(8) Shortest paths	1.10–1.15[l]	$\log_3 3 = 1$	1.145[c]	1.144[c]

[a]The theoretical $\beta/\nu = \frac{5}{48}$ (Ref. 12) yields 1.8958.
[b]Refs. 10 and 11b.
[c]Obtained by renormalization analysis.
[d]Ref. 10c.
[e]Lower and upper bounds by renormalization analysis.
[f]Ref. 4.
[g]Deduced from lines 1 and 7, by Ref. 7 or the rule in Ref. 1 (Table I). $\beta/\nu = \frac{5}{48}$ yields 2.844.
[h]Obtained by Monte Carlo.
[i]Deduced from line 7, by Ref. 8 or the rule in Ref. 1 (Table I).
[j]Deduced from lines 1 and 5, by Refs. 7 and 8 or the rule in Ref. 1 (Table I).
[k]Ref. 8.
[l]Refs. 10a and 11.

able, except for the shortest paths. The model remains attractive because of the utter simplicity of the description and the derivations. The numbers 2, 5, 6, and 8 are also the eigenvalues of the "transfer matrix"[13] describing the fractal.

The random squig clusters of Ref. 1, Figs. 3 and 4 here, described in the paragraph after the next one, are far more realistic. There is one parameter:

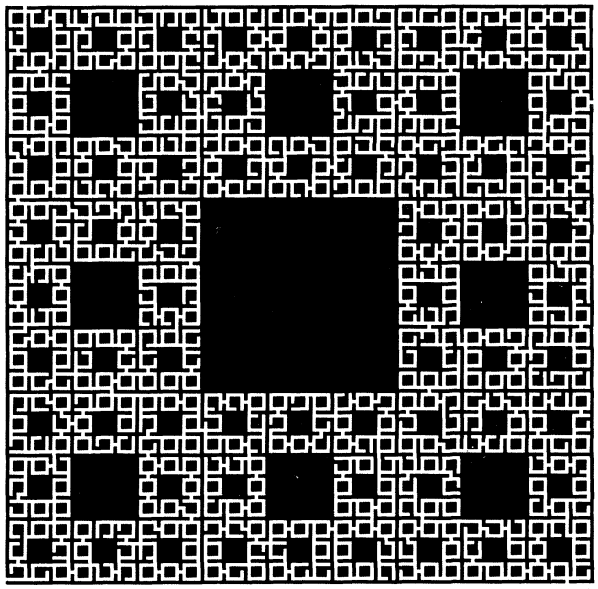

FIG. 3. Negative of a sample of a Ref. 1 cluster, with $b=3$ and $s=0.4$ after three stages.

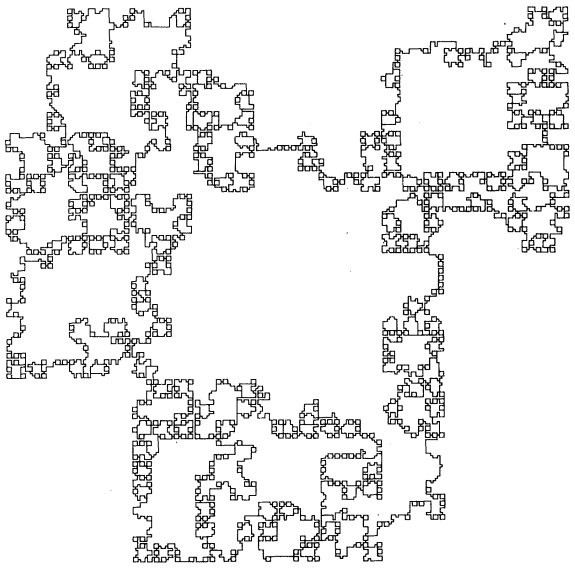

FIG. 4. Sample of the largest ring in the Ref. 1 cluster with $b=3$ and $s=0.4$, after four stages.

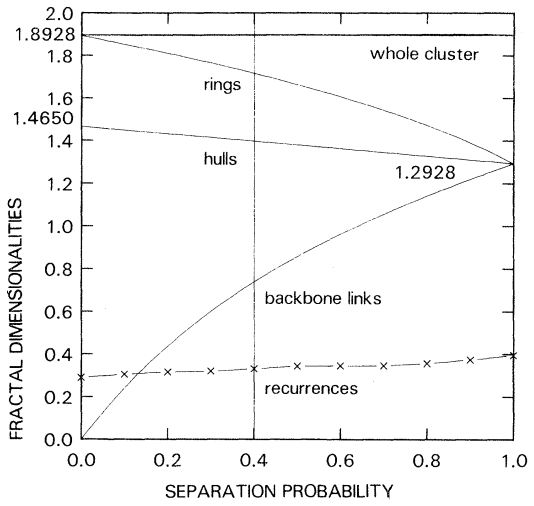

FIG. 5. Dependence upon the separation probability s of the dimensionalities of selected portions of Fig. 3.

the separation probability s. Figure 5 reports various fractal dimensionalities determined either by renormalization analysis (described below) or by Monte Carlo calculation. Our Monte Carlo method used clusters of linear size 3^5, with a few clusters of linear size 3^{10} as a check, averaged over 1000 runs for $s \neq 0.4$ and 2000 runs for $s = 0.4$ as a check. The mean square displacement is $\propto n^{2H}$, the log-log graphs being so straight that $2H$ could be fitted by hand very precisely. The fitted H increases with s. Assuming that the true H fall on a very smooth curve suggests measurement errors below 1%.

Column 5 of Table I reports the dimensionalities of parts of the fully random variant for $s = 0.4$. The fit with column 2 is very satisfactory. It improves further if $s = 0.4 + \epsilon$, but column 2 is not certain enough to pinpoint the best ϵ. Column 4 shows that the half-random variant fits less well, but is a good compromise.

We recall from Ref. 1 the process that generates squig clusters. It begins with the Sierpinski carpet of base $b = 3$, which has the very acceptable fractal dimensionality $\log_3 8 \sim 1.8928$, but is not at all suitable as a model here, since—unlike percolation clusters—the carpet has no dangling bonds and is infinitely ramified (Ref. 2, Chap. 14; Ref. 14). The idea (like in Ref. 13) is to leave the carpet's dimensionality unchanged, while either bonds or sites are deleted recursively. The very versatile "menu" provided by squigs (Ref. 1, Sec. 1; Ref. 2, Chap. 24; and Ref. 15) offers many possibilities.

We work with the carpet's "dual" obtained as follows. After midsquares have been removed, a finite approximation to the carpet is usually a collection of squares, each bounded by four of the usual bonds. The dual sites are centers of these squares, and the dual bonds join the centers of carpet squares that share a side. The approximate dual carpet is the sum of eight subcarpets, each linked to neighbors by many bonds (which is why the carpet is infinitely ramified). To achieve finite ramification, Ref. 1 "decimates" these bonds, i.e., deletes all but one, recursively. The nondeleted bond may be either the central one (half-random version) or selected at random (random version).

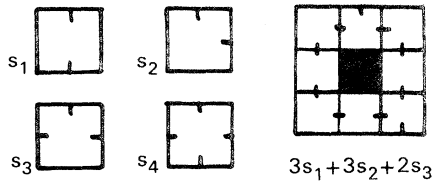

FIG. 6. The four basic shapes in a cluster backbone, a realization of the first-order backbone, and its recursive decomposition.

Next, Ref. 1 creates dangling bonds via a different rule, "separation." The already decimated carpet is made of eight subcarpets, plus eight bonds linking neighboring subcarpets. Random bond separation deletes a nondecimated bond with prescribed probability s, which is the only adjustable parameter in the model. One proceeds in the same way with each part.

By design, the overall dimensionality remains $\log_3 8$, but the topology is made finitely ramified and with dangling bonds. One can prove that point to point backbones' and rings' dimensionalities are identical here.

The case $s = 1$ yields a tree in which the dimensionality of the path joining any two points is 1.2928 (random decimation) or 1.2926 (centered decimation). When $s < 1$, these dimensionalities refer to the path of a random electron through the cluster (Ref. 1. Sec. 1.1.3; thus motivating the above rule of separation by the Kirchhoff laws).

The recursive calculation of the fractal dimensionalities of the basic fractal subsets of a Ref. 1 cluster uses the fractal real-space renormalization group.[16] To illustrate, the cluster backbone involves four basic shapes. For each shape of generation k, draw (Fig. 6) all possible ways of decimating and separating. Each is a linear combination of shapes of order $k+1$. Adding in all possibilities with their correct weights yields for the vector of shapes S a recursion of the form $S' = MS$, where the

transfer matrix[13] M is $M=(1-s)M_1+sM_2$, the matrices M_1 and M_2 resulting, respectively, from nonseparated and separated configurations. By Ref. 17, the backbone's fractal dimensionality is $\log_b\lambda_{max}$, where λ_{max} is the largest eigenvalue of M. A larger space of basic shapes handles our various problems via the eigenvalues of one transfer matrix.

The nonrandom variant with which we started involves a "site separation" roughly equivalent to $s=0.5$. On all levels of iteration except the lowest, the dual sites nearest to the midpoints of the sides of the erased squares are made to reflect a walk reaching them. Next, when two bonds meet at a site, join their midpoints, when three bonds meet, join the midpoints of the bonds that are not collinear. The result is Fig. 2.

In conclusion, the random Ref. 1 clusters with $b=3$ were shown to have very desirable properties, both geometric (fractial and topological) and physical. These new models may also provide workable tests for further problems. Higher-base and higher-dimension variants are available in case of need.

We are grateful to J. H. Cook and R. F. Voss for designing Figs. 3 and 4, to Y. Gefen and A. Aharony for interesting discussions, and to M. E. Fisher for a fruitful comment.

[1]B. B. Mandelbrot, J. Stat. Phys. **34**, 895 (1984).

[2]B. B. Mandelbrot, *The Fractal Geometry of Nature* (Freeman, San Francisco, 1982).

[3]*Percolation Structures and Processes, Annals of the Israel Physical Society, Vol. 5,* edited by G. Deutcher, R. Zallen, and J. Adler (Bar-Ilan University, Ramat-Gan, Israel, 1983); and A. Aharony, J. Stat. Phys. (to be published), are recent surveys. See also D. Stauffer, Phys. Rep. **54**, 3 (1979); S. Kirpatrick, in *Electrical Transport and Optical Properties of Inhomogenous Media—1977,* edited by J. C. Garland and D. B. Tanner, AIP Conference Proceedings No. 40 (American Institute of Physics, New York, 1978), p. 99; A. Coniglio, J. Phys. A **15**, 3829 (1982).

[4]A. Coniglio, Phys. Rev. Lett. **46**, 250 (1981); Y. Gefen, A. Aharony, and B. B. Mandelbrot, J. Phys. A **16**, 1267 (1983).

[5]P. G. de Gennes, Recherche **7**, 919 (1976).

[6]J. A. Given and B. B. Mandelbrot, J. Phys. A **16** L565 (1983).

[7]S. Alexander and R. Orbach, Phys. Rev. Lett. **50**, 77 (1983); R. Rammal and G. Toulouse, J. Phys. (Paris), Lett. **44**, L13 (1983). In the plane, the Alexander-Orbach value $D_{fracton}=\frac{4}{3}$ is questioned by A. Aharony and D. Stauffer, to be published, and by D. C. Hong, S. Havlin, H. J. Hermann, and H. E. Stanley, to be published.

[8]D. Ben-Avraham and S. Havlin, J. Phys. A. **15**, L691 (1982); J. C. Angles d'Auriac, A. Benoit, and R. Rammal, J. Phys. A **16**, 4039 (1983).

[9]Y. Gefen, A. Aharony, and S. Alexander Phys. Rev. Lett. **50**, 77 (1983).

[10a]L. Peuch and J. Rammal, J. Phys. C **16**, 4197 (1983); P. S. Li and W. Streider, J. Phys. C **15**, L1235 (1982).

[10b]H. J. Herrmann, D. C. Hong, and H. E. Stanley, J. Phys. A **17**, L261 (1984).

[10c]R. F. Voss, to be published.

[11a]R. Pike and H. E. Stanley, J. Phys. A **14**, L169 (1982).

[11b]D. C. Hong and H. E. Stanley, J. Phys. A **16**, L475, L525 (1983).

[11c]S. Havlin and R. Nossal, J. Phys. A (to be published).

[12]B. Nienhuis, J. Phys. A **15**, 199 (1982).

[13]B. B. Mandelbrot, Y. Gefen, A. Aharony, and J. Peyiére, to be published.

[14]Y. Gefen, B. B. Mandelbrot, and A. Aharony, Phys. Rev. Lett. **45**, 855 (1980); Y. Gefen, A. Aharony, B. B. Mandelbrot, and S. Kirkpatrick, Phys. Rev. Lett. **47**, 1771 (1981).

[15]B. B. Mandelbrot, C. R. Acad. Sci., Ser. A **286**, 933 (1978), and Recherche **9**, 1 (1978), and in Proceedings of the Fractals Conference, Gaithersburg, Maryland, 1983 [J. Stat. Phys. (to be published)]. A variant is found in D. J. Klein and W. A. Seitz, Proc. Nat. Acad. Sci. U.S.A. **80**, 3125 (1983).

[16]J. A. Given and B. B. Mandelbrot, in Proceedings of the Fractals Conference, Gaithersburg, Maryland, 1983 [J. Stat. Phys. (to be published)].

[17]J. Peyriére, C. R. Acad. Sci., Ser. A **286**, 937 (1978), and Ann. Inst. Fourier **31**, 187 (1981).